Plasma density behavior with new graphite limiters in the Hefei Tokamak-7

M. Asif,[a] X. Gao, J. Li, G. L. Kuang, B. N. Wan, Y. X. Jie, J. Y. Zhao, X. D. Zhang, H. Q. Liu, X. D. Tong, J. Liu, Q. Xu, J. S. Hu, Y. Yang, B. Shen, J. S. Mao, L. Q. Hu, Z. W. Wu, B. L. Ling, and the HT-7 Team
Institute of Plasma Physics, Chinese Academy of Sciences, P.O. Box 1126, Hefei, Anhui 230031, People's Republic of China

(Received 3 May 2005; accepted 17 June 2005; published online 21 July 2005)

A new set of actively cooled toroidal double-ring graphite limiters has been developed in the Hefei Tokamak-7 (HT-7) [X. Gao *et al.*, Phys. Plasmas **7**, 2933 (2000)] for long pulse operation. The extension of operational region and density behavior with graphite (C) limiters have been studied in this paper. Extended high-density region at the high plasma current low-q_a was obtained. The density profile with the C limiter was studied to compare with the previous molybdenum (Mo) limiter. The critical density of multifaceted asymmetric radiation from the edge (MARFE) onset is observed in the region of $Z_{eff}^{1/2} f_{GW}=0.9\sim 1.2$, where $f_{GW}=\bar{n}_e/n_{GW}$. (Here $\bar{n}_e$ is the maximum line average electron density and n_{GW} is the Greenwald density.) Under the same injected power, the critical density of MARFE onset with the new C limiter is much higher than the previous Mo limiter. © *2005 American Institute of Physics*. [DOI: 10.1063/1.1995627]

I. INTRODUCTION

Many machines were operated for the mixed carbon material used for long pulse operation, ultimately steady state. The graphite-based first wall components have been designed and tested to sustain particle and heat exhausts under steady-state conditions in Tore Supra.[1] After plasma operation, it appears that the components and the brazing techniques must be optimized, especially through the use of more thermal shock-resistant materials as carbon fiber composites.[2] A major part of the DIII-D[3] program is focused upon high performance experiments. DIII-D was operated successfully with an all-graphite wall, dramatically reducing metal impurity accumulations without increasing the influx of low-Z impurities. HT-7 is a superconducting tokamak[4] with the limiter configuration designed to operate with high power and long duration discharge. The last closed flux surface was defined by the main poloidal limiter in 1999, which receives the highest heat loads and largest flux of energetic particles bombardment from the plasma. In past operations with the Mo limiter, due to energetic particles bombardment and overheating problem, the plasma discharge was usually terminated by the very strong hard x-ray radiation, hot spot and high-Z impurities. It has been reported earlier that the siliconization[5] did not allow a large increase in the available pulse length with Mo limiters. However, the impurity level was reduced significantly, and plasma performance was improved after ion cyclotron resonance frequency (ICRF) siliconization. In order to alleviate the above problems, a new set of actively cooled toroidal double-ring graphite limiters (see Fig. 1), has been developed in the Hefei Tokamak-7 (HT-7) superconducting tokamak in 2004. The doped graphite GBST1308 with the dopant concentration of 1% B, 2.5% Si, 7.5% Ti (about 20% of first wall) was used as limiter material.[6] It has high thermal conductivity up to 210 W/mK. Its good thermal shock resistance can withstand 6 MW/m^2 high heat loads for long pulse operation. The evaluation of thermal performance of doped graphite GBST1308 under steady-state high-heat flux was carried out in ACT (actively cooling test stand) of the National Institute for Fusion Science. Details of steady high heat flux experiments were described in the paper.[7] There was no obvious surface damage on the surface of the new carbon limiter after tokamak experiments. Very stable and reproducible discharges were obtained with significantly increased density and a large increase in the available pulse length, as compared to Mo limiters. Up to 240 s of long pulse discharge has been achieved by lower hybrid current drive with new graphite limiters in the HT-7 in 2004. The operation parameter space is largely expanded, and the edge recycling, plasma density and impurity can be easily handled. The operational regime and density behavior with new graphite limiters were studied in this paper. The extension of the HT-7 operational region has been reported. The density limit and the multifaceted asymmetric radiation from the edge (MARFE) phenomena on high-density operation were compared between new graphite (C) limiter and previous molybdenum (Mo) limiter in the Hefei Tokamak-7 (HT-7) superconducting tokamak, and have been summarized in this paper.

II. EXPERIMENTAL SETUP

The Hefei Tokamak-7 (HT-7) is a superconducting tokamak,[4] and it was reconstructed from the original Russian T-7 tokamak in 1994. It has a major radius of $R=1.22$ m, minor radius of $a=0.27$ m in the circular cross section. There are two layers of thick copper shells, and between them are located 24 superconducting coils which can create and maintain a toroidal magnetic field (B_T) of up to 2.5 T. Based on the understanding of plasma surface interactions, several technical improvements have been made recently. The new GBST1308 doped graphite was used as limiter material. All

[a]Electronic mail: asif@ipp.ac.cn

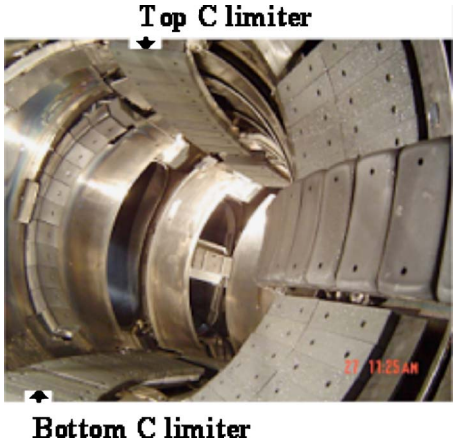

FIG. 1. A new set of actively cooled toroidal double-ring graphite limiters at the bottom and top of the vacuum vessel on HT-7 tokamak in 2004.

carbon tiles were coated with 100 μm silicon carbide (SiC) functional gradient coating.[6] The two poloidal water-cooling limiters and one toroidal water-cooling belt limiter at high field side were developed in 2002.[6] A new set of actively cooled toroidal double-ring graphite limiters at the bottom and top of the vacuum vessel was developed recently, as shown in Fig. 1, for long pulse operation, and up to 240 s of long pulse plasma has been achieved in the HT-7 in 2004 as shown in Fig. 2.

The major research fields on the HT-7 are steady-state operation, high-performance such as advanced tokamak operation modes, the fueling study[8] and MARFE phenomena,[9] lower hybrid wave current drive[10] and ICRF heating.[11] For recent experiments on the HT-7, the following main diagnostics signals are effectively used in this paper: a 16-channel XUV bolometer array to measure plasma radiation losses, a 7-channel bremsstrahlung emission ($Z1\sim7$) to measure Z_{eff}, a multichannel $H_\alpha(D_\alpha)$ radiation array, 10-channels CIII line emission, an impurity optical spectrum measurement system and the electron density profile measured by a vertical 5-channel far-infrared hydrogen cyanide (HCN) laser interferometer.[12,13] The laser source used in the interferometer was a continuous-wave DC glow discharge HCN laser with 3.4 m cavity length and 100 mW power output at 337 μm wavelength. The system has a temporal resolution of 0.1 ms with a 10 kHz rotating grating.[13]

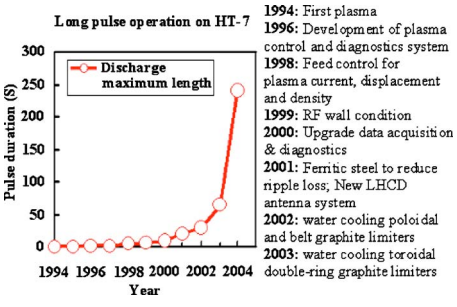

FIG. 2. Progress of long-pulse operation in the HT-7 tokamak.

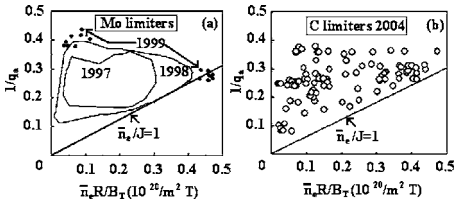

FIG. 3. Hugill plot for HT-7 superconducting tokamak with: (a) molybdenum, and (b) graphite limiters.

III. HIGH DENSITY OPERATION

The density limit problem has been tackled since 1970, but a unique physics picture has not emerged so far. The first density limit trend was outlined by Murakami in 1976:[15] the maximum line average electron density ($\bar{n}_e$) achieved by several machines appeared to scale as the ratio between the toroidal field (B_T) and the plasma major radius (R). Following the extension of the tokamak operation range, it was pointed out by Hugill and co-workers that the normalized average density $\bar{n}_e R/B_T$ scaled as the inverse safety factor $1/q$. For a circular plasma, the quantity $1/q$ is proportional by definition to JR/B_T, where J is the average plasma current density $I_P/\pi a^2$ (where a is the minor radius of plasma): this suggests that by eliminating the dependence on B and R, the Hugill limit would appear in the form $\bar{n}_e$ proportional to J. In 1988, Greenwald[16] showed that in elongated tokamaks the relevant parameter remains the "circular equivalent" safety factor ($q_c = 5a^2 B_T/\mu_0 R I_P$); thus, the maximum achieved densities scale as $\bar{n}_e = \kappa J$, where $\kappa = b/a$ is the elongation and $J = I_P/\pi ab$ is the average current density in the new geometry. From the large amount of the available tokamak data, a proportionality factor of unity was found between density $\bar{n}_e$, expressed in units of 10^{20} m^{-3}, and J, expressed in units of MA/m^2. In the last few years, owing to better diagnostics, especially for the plasma edge, the use of pellet injectors to fuel the plasma and the experience gained on many different tokamaks, a consensus has been reached on the edge density being the real parameter responsible for the density limit.[17–19] There are two main mechanisms invoked to explain this limit: one refers to the power balance between the heat conducted and/or convected across the plasma radius and the power lost by impurity line radiation at the edge;[20] the other explanation is based on the particle and energy balance in the scrape-off layer (SOL), which imposes a limit on the edge density associated with the thermal collapse of the SOL plasma.[21] In the HT-7 tokamak, the density limit appeared to be connected with the impurity content and the

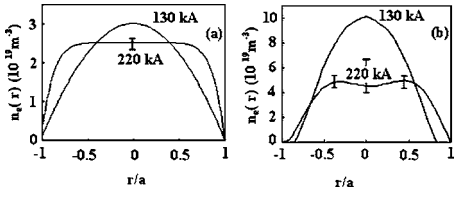

FIG. 4. Electron density profiles reaching the same average density at same toroidal field ($B_T \sim 2$ T) with (a) molybdenum and (b) graphite limiters.

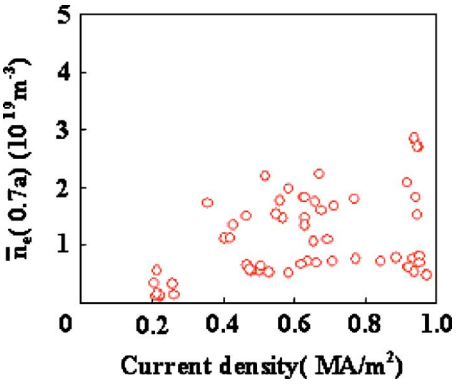

FIG. 5. Density at the magnetic surface with 22% of the maximum flux ($r/a \cong 0.7$) versus the average current density.

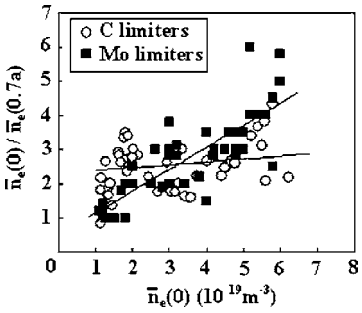

FIG. 6. Peaking factor $\bar{n}_e(0)/\bar{n}_e(0.7a)$ with different line averaged-density conditions in the HT-7 graphite and molybdenum limiters.

edge parameters, and the best results were obtained with very clean plasmas and the peaked electron density profiles.

The HT-7 tokamak is normally operated with $I_P = 100$–250 kA, $B_T = 1$–2.5 T, line-averaged density 1–6 $\times 10^{19}$ m^{-3}. The first plasma was produced on the HT-7 superconducting tokamak in 1994,[22] and the operation region of the HT-7 Ohmic discharges were limited by the wall condition and the HT-7 controlling system before 1997 as shown in Fig. 3. During the Spring experimental campaign in 1998, a feedback control system to simultaneously control plasma current, density and displacement was developed and put into daily operation. Figure 3 shows the Hugill plot of the data taken during this phase, together with the HT-7 experimental limit corresponding to an inverse slope $\bar{n}_e R q_a / B_T = 1.61 \times 10^{20}\ Wb^{-1}$: this line also represents the Greenwald limit[16] $\bar{n}_e/J = 1$, where $\bar{n}_e$ and J are measured in units of 10^{20} m^{-3} and MA/m^2, respectively. Since 1998 the radio frequency (RF) wave boronization, a new technique for the superconducting tokamak wall conditioning, has been successfully developed on the HT-7.[14] The pulsed radio frequency plasma was produced by a non-Faraday shielding RF antenna with RF power of 10 kW at 30 MHz in the toroidal field B_T of 1.8 T, and solid carborane powder which is nontoxic and nonexplosive was used under the pressure of 3 $\times 10^{-1}$ Pa. In Fig. 3, the solid points (at the high-density region and the high-current low-q_a region) were achieved by the RF boronization and the RF siliconization, respectively, in 1999.[14] During the Spring experimental campaign in 2004, a new set of actively cooled toroidal double-ring graphite limiters at the bottom and top of the vacuum vessel has been developed as shown in Fig. 1, for long pulse operation in the HT-7. Figure 3 shows the Hugill plot of the data taken during this phase, along with the previous molybdenum limiter at a range of $B_T = 1$–2.5 T. In Fig. 3, the extended high-density region at the low-q_a was achieved. It was clear that the new C limiters extended both the operational parameter space as shown in Fig. 3 and discharge length as shown in Fig. 2 on the HT-7 tokamak.

In all the explored q range (or J range for fixed geometry and field), the Murakami parameter is shown in Fig. 3, for Mo and C limiter materials. While the limited range accessible to operation could be explained by a substantial content of light impurities (oxygen and carbon) and their consequent effect on the radiation losses, it was more surprising to find an apparent lack of dependence of the density limit on the plasma current. From closer inspection of the data, it turns out that the density profiles at higher current were systematically broader than those at low current as shown in Fig. 4, for Mo and C limiter materials, especially in the vicinity of the density limit, so this picture changed substantially if one looked at the edge density as the limiting parameter. In the absence of a direct measurement of the edge density, we took as an indication the edge line averaged density, $\bar{n}_e(0.7a)$ at the magnetic surface, the poloidal flux Ψ satisfying

$$\Psi - \Psi_{\text{edge}} = 0.22(\Psi_0 - \Psi_{\text{edge}})$$

where Ψ_0 is the flux at the magnetic axis. Typically, this corresponds to a relative radial position of 0.7. In Fig. 5, the $\bar{n}_e(0.7a)$ versus current density was shown for the data of Fig. 3. In this plot, the current density dependence appears, thus suggesting that when the central chord average density is plotted, it is canceled by the profile effect. The density limit appeared to be connected with the edge parameters in the HT-7. The density profile with C limiter was studied to compare with previous Mo limiter. Figure 6 shows the peaking factors $\bar{n}_e(0)/\bar{n}_e(0.7a)$ [where $\bar{n}_e(0)$ is the line average density, measured at the central interferometer channel at $r = 0$ cm and $\bar{n}_e(0.7a)$ is the line average density, measured at the outermost interferometer channel at $r = 20$ cm ($r = 0.7a$, the minor radius $a = 27$–28 cm)], for different averaged-density conditions, and the higher density always correlated with the peaked profile in the HT-7. Comparing with the previous molybdenum material limiter, it is observed that the peaking factor of the electron density profile is weakly pro-

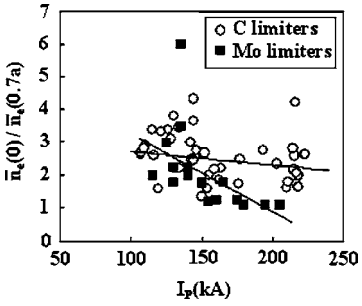

FIG. 7. Peaking factor $\bar{n}_e(0)/\bar{n}_e(0.7a)$ of the density profiles with different plasma current I_P in the HT-7 graphite and molybdenum limiters.

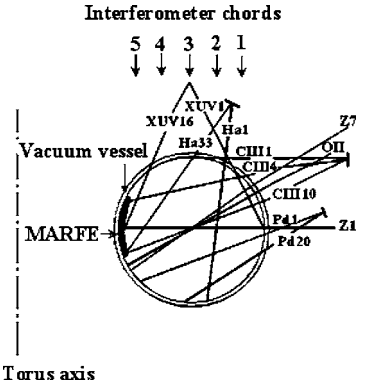

FIG. 8. A chord view of the vertical 5-channel HCN interferometer (from low field to high field at +20 cm, +10 cm, 0 cm, −10 cm, −20 cm), 20-channel H_α emission (Pd1～20), 33-channel H_α emission, 10-channel CIII emission, 7-channel bremsstrahlung emission (Z1～7), 16-channel XUV bolometer, one channel OII line emission chord in the HT-7 tokamak.

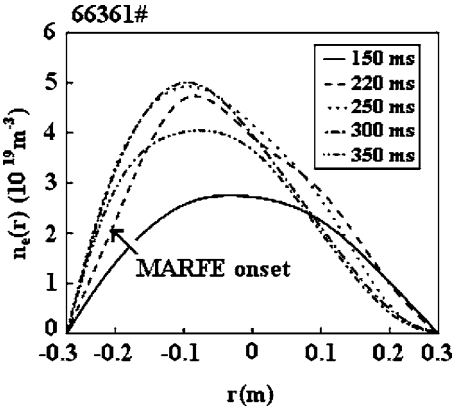

FIG. 10. Electron density profiles $n_e(r)$ by Abel inversion (at t=150 ms, 220 ms, 250 ms, 300 ms and 350 ms).

portional to the line average density with the graphite limiter. Figure 7 shows the peaking factor of the density profiles for different plasma currents, and the peaked profiles were obtained at high current range of I_P=120–220 kA. Comparing with the Mo limiter data, higher density and its peaked profile were achieved on high plasma current discharges by new graphite limiters, which led to extension of the operational region, as shown in Fig. 3.

IV. MARFE

The multifaceted asymmetric radiation from the edge (MARFE)[23–25] is poloidally asymmetric but toroidally symmetric regions of locally high density, low temperature plasmas located on the high field side, give rise to strong radiation. The MARFE phenomenon usually appears beyond a critical density in the tokamaks. In the HT-7 superconducting tokamak with the molybdenum limiter, the onset of a MARFE usually occurs in the early Ohmic discharges (Z_{eff}=3–8 and 15%–25% of the Greenwald density limit scaling[16] for circular plasmas: $n_{GW}=I_P/\pi a^2$, where n_{GW} is in the units of 10^{20} m^{-3}) of each experimental campaign before wall conditioning. The occurrence and location of a MARFE is identified by different diagnostic systems as shown in Fig. 8. There is no significant increase in concentration of oxygen during onset of MARFE with molybdenum limiters and different locations of MARFE are observed for molybdenum limiters.[24] Figure 9 shows the typical shot of experimental campaign 2004 (shot No. 66361) on HT-7 with graphite limiters, the plasma current about 130 kA, the loop voltage $V_{\text{loop}}<3$ V, the toroidal field B_T=1.7 T, Z_{eff}=2.5, R=1.22 m, a=0.27 m and the line-averaged density about 4.5×10^{19} m^{-3}. A typical position of the MARFE on the HT-7 (shot No. 66361) is identified by visible CIII line emission as shown in Fig. 8. The MARFE occurs in the plasma column on the inner high field side. The MARFE onset is characterized by a sudden modification of visible CIII line emission signal. It is clear that MARFE event occurs from t=220 ms suddenly as shown in Fig. 9. In HT-7 graphite limiters, the critical density of MARFE onset is observed in the region of $Z_{eff}^{1/2}f_{GW}$=0.9–1.2, where $f_{GW}=\bar{n}_e/n_{GW}$. (Here $\bar{n}_e$ is the maximum line average electron density and n_{GW} is the Greenwald density.) An asymmetric and peaked density profile is observed as shown in Fig. 10. Under the same injected power, the critical density with the C limiter is much higher than the Mo limiter. The critical conditions for the occurrence of a MARFE in HT-7 can be deduced from the experimental data in the Fig. 11 for limiter materials (molybdenum[24] and graphite). The best correlation has been found between the total input Ohmic power and the product

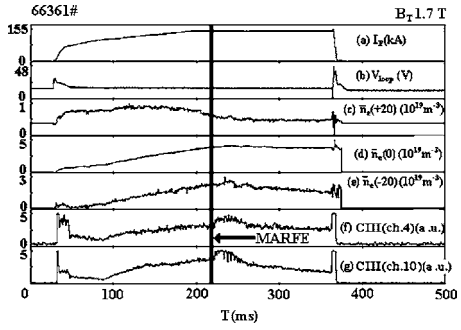

FIG. 9. The onset of a MARFE in the HT-7: (a) plasma current, (b) loop voltage, (c) line averaged electron density (vertical chord at r=+20 cm), (d) line averaged electron density (vertical chord at r=0 cm), (e) line averaged electron density (vertical chord at r=−20 cm), (f) CIII emission from channel 4, (g) CIII emission from channel 10.

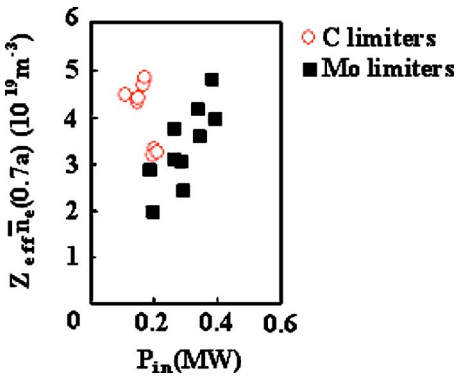

FIG. 11. The critical conditions for the MARFE activity with different limiter materials C and Mo in the HT-7 tokamak.

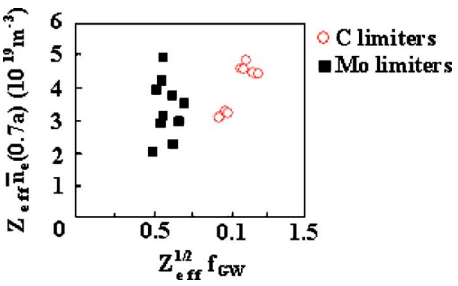

FIG. 12. MARFE occurs at values of $Z_{eff}^{1/2}f_{GW}$ in the range of 0.9–1.2 on new graphite limiters, where $f_{GW}=\bar{n}_e/n_{GW}$. (Here $\bar{n}_e$ is the maximum line average electron density and n_{GW} is the Greenwald density.)

of the line average density, measured at the outermost interferometer channel at $r=20$ cm ($r/a\cong 0.7$, the minor radius $a=27$–28 cm), and Z_{eff}. In the HT-7 tokamak high-Z_{eff} discharges, it is found that the MARFE occurs at values of $Z_{eff}^{1/2}f_{GW}$ in the range of 0.5–0.7 with the molybdenum limiter.[24] The critical factor of MARFE onset is 0.9–1.2 with graphite limiters as shown in Fig. 12. It implies that the MARFE event can occur only at high density and low input Ohmic power discharges with graphite limiters. In future experiments, we will try these discharges with high input power.

A quantitative comparison of impurity reduction via density is shown in Fig. 13 for Mo and C limiter materials. The main impurities were reduced in the case of graphite limiters. The density limit appeared to be connected with the impurity content (see Fig. 13) and the edge parameters, and the best results, significantly increased density and a large increase in the available pulse length was obtained. Moreover, very clean plasmas and the peaked electron density profiles were observed (see Fig. 7).

The MARFE phenomenon usually develops before reaching the density limit.[24] It was found recently that MARFEs typically occur at a fraction, 50–90 %, of the density limit on tokamaks.[26] However, in the HT-7 tokamak the occurrence of a MARFE is not only correlated with the density but also with Z_{eff}.

V. CONCLUSION

A new set of actively cooled toroidal double-ring graphite limiters has been developed in the HT-7 superconducting tokamak for long pulse operation. Significant progress of long pulse operation with a graphite limiter is achieved in the HT-7 as shown in Fig. 2. An extended operational region is obtained with new C limiters. High-density plasma behaviors and the high-density operation region were studied in the HT-7 superconducting tokamak with new graphite limiters. The density profile with the C limiter was studied to compare with the previous Mo limiter. The peaking factor of electron density profile is weakly proportional to the line average density with C limiters. In the HT-7, the best correlation has been found between the total input Ohmic power and the product of the edge line average density and $Z_{eff}^{1/2}$. In HT-7 with graphite limiters, the critical density of MARFE onset is observed in the region of $Z_{eff}^{1/2}f_{GW}=0.9$–1.2 as shown in Fig. 12. Under same injected power, the critical density with the C limiter is much higher than the Mo limiter.

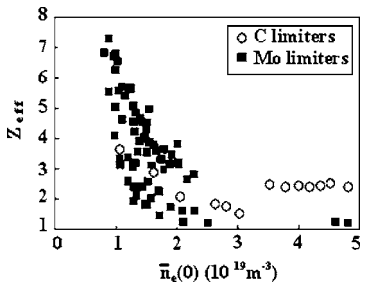

FIG. 13. Comparison of impurity content with graphite and molybdenum limiter materials, in the HT-7 tokamak.

ACKNOWLEDGMENTS

The authors wish to thank the HT-7 team for cooperation during these experiments.

This work has been supported by the National Natural Science Foundation of China (Contract No. 10005010).

[1] M. Lipa, P. Chappuis, and P. Deschamps, Fusion Technol. **19**, 2041 (1991).
[2] Tore Supra team (presented by J. J. Cordier), Fusion Eng. Des. **61-62**, 71 (2002).
[3] G. L. Jackson, D. R. Baker, K. L. Holtrop, S. Konoshima, R. Maingi, G. M. Staebler, and W. P. West, J. Nucl. Mater. **220-222**, 173 (1995).
[4] X. Gao, Y. X. Jie, Y. Yang, C. Y. Xia, M. S. Wei, S. Y. Zhang, Y. F. Cheng, L. Q. Hu, J. S. Mao, X. D. Tong, B. N. Wan, G. L. Kuang, J. G. Li, Y. P. Zhao, J. R. Luo, N. Qiu, K. Yang, G. Li, J. K. Xie, and Y. X. Wan, Phys. Plasmas **7**, 2933 (2000).
[5] X. Z. Gong, J. G. Li, B. N. Wan, Y. P. Zhao, X. D. Zhang *et al.*, J. Nucl. Mater. **290-293**, 1171 (2001).
[6] X. Gao, J. Li, Y. Yang, J. K. Xie, J. R. Luo, J. Y. Zhao, X. Z. Gong, L. Q. Hu, X. D. Zhang, Y. J. Shi, B. N. Wan, K. Tanaka, R. Sakamoto, Y. P. Zhao, G. L. Kuang, J. S. Hu, M. Asif, Y. X. Jie, H. Q. Liu, J. Liu, Q. Xu, L. Gao, and The HT-7 Team, J. Nucl. Mater. **337–339**, (2005) 835.
[7] J. Chen, J. Li, N. Noda, Y. Kubota, Q. Guo, and L. Qiu, Plasma Sci. Technol. **4**, 1387 (2002).
[8] Y. Yang, Y. Bao, J. G. Li, X. M. Gu, and Y. X. He, Nucl. Fusion **39**, 1871 (1999).
[9] X. Gao, Y. P. Zhao, J. R. Luo, Y. X. Jie, X. Z. Gong, B. N. Wan, J. G. Li, F. X. Yin, G. L. Kuang, X. D. Zhang, N. Qiu, X. N. Liu, J. Y. Zhao, Y. Yang, Y. Bao, B. L. Lin, Z. W. Wu, Y. D. Li, Y. H. Xu, K. Yang, G. X. Wang, W. W. Ye, L. Chen, Y. J. Shi, M. Song, X. M. Zhang, P. J. Qin, X. M. Gu, N. Z. Cui, H. Y. Fan, S. X. Liu, Y. F. Chen, L. Q. Hu, J. S. Hu, C. Y. Xia, H. L. Ruan, X. D. Tong, J. S. Mao, J. K. Xie, and Y. X. Wan, Plasma Phys. Controlled Fusion **41**, 1349 (1999).
[10] G. L. Kuang, Y. Liu, J. Shan, W. Xu, X. Zhang, D. Liu, Y. B. Zhu, C. Zhang, G. Zheng, J. Wu, J. Lin, B. Ding, H. Xu, Y. D. Fang, J. G. Li, J. R. Luo, X. D. Zhang, B. N. Wan, Q. Zhao, J. S. Mao, X. Gao, and S. Y. Zhang, Nucl. Fusion **39**, 1769 (1999).
[11] Y. P. Zhao, J. G. Li, J. K. Xie, Y. D. Meng, X. C. Wu, Y. X. He, D. Y. Xue, X. Deng, and Y. G. Shao, Chin. Phys. Lett. **14**, 916 (1997).
[12] X. Gao, H. J. Lu, Q. L. Guo, Y. X. Wan, and X. D. Tong, Rev. Sci. Instrum. **66**, 139 (1995).
[13] Y. X. Jie, X. Gao, Y. F. Cheng, K. Yang, and X. D. Tong, Int. J. Infrared Millim. Waves **21**, 1375 (2000).
[14] J. Li, Y. P. Zhao, X. M. Guo, C. F. Li, B. N. Wan, X. D. Zhang, J. R. Luo, X. Z. Gong, J. K. Xie, Y. X. Wan, P. J. Qin, X. M. Wang, Y. D. Meng, S. F. Li, X. Gao, Y. Yang, D. Y. Xue, Y. Z. Mao, X. Den, L. Chen, Y. C. Fang, F. X. Yin, S. X. Liu, X. K. Yang, D. Z. Xu, J. Y. Ding, Y. X. Jie, Q. C. Zhao, J. S. Mao, S. Y. Zhang, J. Y. Zhao, J. S. Hu, H. Y. Fan, M. S. Wei, B. L. Lin, G. X. Wang, Y. D. Fang, and W. C. Shen, Nucl. Fusion **39**, 973 (1999).
[15] M. Murakami, J. D. Callen, and L. A. Berry, Nucl. Fusion **16**, 347 (1976).
[16] M. Greenwald, J. L. Terry, S. M. Wolfe, S. Ejima, M. G. Bell, S. M. Kaye, and G. H. Neilson, Nucl. Fusion **28**, 2199 (1988).

[17]D. Frigione, L. Pieroni, V. Zanza, G. M. Apruzzese, F. Alladio, M. L. Apicella, R. Bartiromo, M. Borra, G. Bracco, G. Buceti, P. Buratti, C. Centioli, M. Ciotti, V. Cocilovo, I. Condrea, F. Crisanti, R. De Angelis, B. Esposito, A. Frattolillo, G. Gatti, E. Giovannozzi, G. Granucci, M. Grolli, A. Imparato, H. Kroegler, M. Leigheb, L. Lovisetto, G. Maddaluno, G. Mazzitelli, P. Micozzi, S. Migliori, A. Moleti, F. Orsitto, D. Pacella, L. Panaccione, M. Panella, V. Pericoli-Ridolfini, S. Podda, G. B. Righetti, E. Sternini, A. A. Tuccillo, O. Tudisco, F. Valente, V. Vitale, and M. Zerbini, Nucl. Fusion **36**, 1489 (1996).
[18]Y. Kamada, N. Hosogane, R. Yoshino, T. Hirayama, and T. Tsunematsu, Nucl. Fusion **31**, 1827 (1991).
[19]A. Stabler, K. McCormick, V. Mertens, E. R. Muller, J. Neuhauser, H. Nedermeyer *et al.*, Nucl. Fusion **32**, 1557 (1992).
[20]J. A. Wesson, R. D. Gill, M. Hugon, F. C. Schuler *et al.*, Nucl. Fusion **29**, 641 (1989).
[21]K. Borrass and the NET Team, Nucl. Fusion **33**, 63 (1993).
[22]J. K. Xie and the HT-7 group, *Proceedings of the 16th International Conference on Plasma Physics and Controlled Nuclear Fusion Research, Montreal, Plasma Physics Controlled Nuclear Fusion Research 1996* (International Atomic Energy Agency, Vienna, 1997), Vol. 1, p. 685.
[23]B. Lipschultz, B. Labombard, E. S. Marmar, M. M. Pickrell, J. L. Terry, R. Watterson, and S. M. Wolfe, Nucl. Fusion **24**, 977 (1984).
[24]X. Gao, J. R. Luo, Y. P. Zhao, N. Qiu, Y. X. Jie, Y. Yang, C. Y. Xia, B. N. Wan, G. L. Kuang, X. D. Zhang, J. G. Li, F. X. Yin, X. N. Liu, X. Z. Gong, S. Y. Zhang, J. Y. Zhao, and L. Q. Hu, J. Nucl. Mater. **279**, 330 (2000).
[25]M. Asif, X. Gao, J. G. Li, and B. N. Wan, Phys. Lett. A **336**, 61 (2005).
[26]B. Lipschultz, J. L. Terry, C. Boswell, A. Hubbard, B. Labombard, and D. A. Pappas Phys. Rev. Lett. **81**, 1007 (1998).